

Mechanics of the Extension of Cotton Fibers. II.

Theoretical Modeling

J. W. S. HEARLE and J. T. SPARROW, *Department of Textile Technology, University of Manchester Institute of Science and Technology, Manchester, England*

Synopsis

A preliminary analysis of deconvolution of a nylon model is given. This is then developed to give the available deconvolution strain in cotton. The total extension is then given by adding the fibrillar strain and is compared with experimental values of breaking extension. The relation between convolution extension and stress is calculated in terms of structural and mechanical parameters. An earlier analysis derived cotton fiber modulus in terms of fibril extension and volume change. A new analysis shows that the introduction of shear resistance does not have a significant effect when rotation is prevented. However, false untwisting can occur at the helix reversal in cotton fibers. An analysis which allows for this rotation shows a strong dependence on shear modulus as well as fibril extension and helix angle. There is no volume change.

INTRODUCTION

As indicated in the introduction to part I, the earlier theoretical analysis of the extension of cotton and other plant fibers by Hearle^{1,2} has applied the methods of twisted yarn mechanics and treated the fiber as a solid assembly of molecularly oriented fibrils arranged on helical paths around the axis of a circular cylinder. Although the predictions show results in general agreement with experimental observations of the form of change of modulus over a wide range of spiral angles, there is an uncertainty by a factor of about two in the modulus value at zero angle, a lack of agreement for the differences between cotton varieties, and no explanation of the shape of the cotton fiber stress-strain relation, which curves upwards at low strains to become stiffer as extension proceeds and becomes more linear at high strains.

Furthermore, the model ignores a number of structural features of the cotton fiber which are clearly of importance. First, there is an implicit assumption in twisted yarn mechanics that individual fibers can slide past one another to relieve local shear strains. In a well-bonded solid material this cannot happen, although with weak intermolecular bonding there might be internal slippage and loss of continuity. The contribution of shear energy needs to be taken into account, since, if appreciable, it would stiffen the fibers. Second, there is an implicit assumption in most twisted yarn mechanics that the extension occurs without any twisting or untwisting of the yarn. Untwisting would tend to occur because it causes an increase of length, thus relieving tensile stress, but it is prevented by the clamping of the twisted yarn specimen at each end. However, in the cotton fiber, because of the reversals, both twist directions are present, and "false untwisting" can occur at reversal points: the analysis should therefore be that in which free untwisting is allowed. Both of these effects were mentioned in a

more recent paper on yarn mechanics³ and should certainly be brought into the analysis for cotton fibers. However, the fiber problem is simpler in that it is reasonable to take the helix angle as constant through the fiber, instead of varying as in yarns, and the analysis can be limited to small strains and Hookean elasticity. It is therefore convenient to do the analysis independently.

The third feature, confirmed experimentally in part I, is the importance of the fact that the cotton fiber is a convoluted ribbon. The removal of the convolutions contributes substantially to the extension at low stresses.

A full mechanical analysis of a convoluted ribbon, with fibrils following distorted and flattened helical paths, would be difficult. The problem is simplified by separating the extension into two parts: (1) the strain due to deconvolution; and (2) the strain due to extension of a freely untwisting helical assembly, assumed for simplicity to be circularly cylindrical, solid, and of constant helix angle.

Apart from errors due to differences between flattened and circular geometry in calculating the second point, this treatment ignores (a) any contribution from the primary wall; (b) any effect of the changes in helix angle which occur through the secondary wall; (c) any specific localized strains at the reversal points; (d) any effect of the residual lumen; (e) any effect of the disturbance of the fine structure on collapse of the fiber; and, indeed, (f) any differences from a fine structure which is assumed to consist of crystalline cellulose oriented perfectly along the helical lines. However, none of these factors would be expected to have a large effect on the extension behavior (though they may influence fracture, which is dependent on local extremes rather than averages), and so they are reasonably neglected.

THEORETICAL ANALYSIS OF DECONVOLUTION

Nylon Model

It was shown in part I that a ribbon of nylon, which has been set in a twisted form and which has equal lengths of S and Z twist separated by a reversal, exhibits a decreasing initial modulus as the amount of twist per unit length increases. It was also shown that as the twist per unit length increases, the extensibility increases. The increase in extensibility is due to a deconvolution or untwisting effect.

Timoshenko⁴ has derived the following equation for the contraction in length of a thin rectangular strip during twisting:

$$\epsilon = \frac{\phi^2 b^2}{2 \cdot 12} - \frac{\delta}{Y} \quad (1)$$

where ϵ is the strain, ϕ is the twist in radians per unit length, b is the ribbon width, δ is the longitudinal stress acting on the strip, and Y is the Young's modulus of the material. When a ribbon is twisted, there will be tensile forces at the outer edges and compressive forces at the center. The above relation takes account these forces.

We can apply eq. (1) to the untwisting of a strip with initial twist ϕ_0 and say that

$$\epsilon_c = \phi_0^2 b^2 / 24 \quad . \quad (2)$$

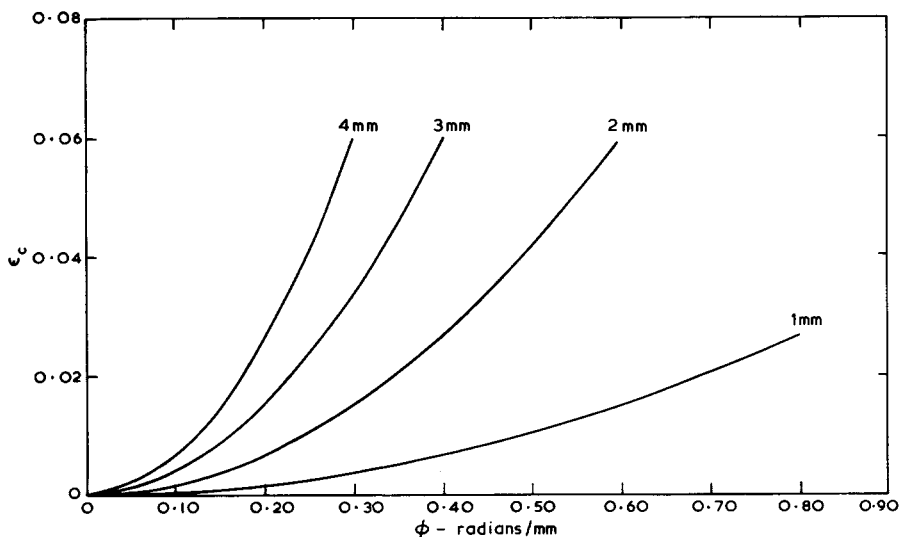


Fig. 1. Variation of deconvolution strain ϵ_c with twist and ribbon width as calculated from eq. (2).

TABLE I
Calculated and Measured Deconvolution Strain of Nylon Strips

Twist (rad/mm)	ϵ_c [from eq. (2)]	ϵ_c , actual (from Fig. 4 of part I)
0.100	0.0016	0.0010
0.207	0.0072	0.0060
0.314	0.0164	0.0140
0.378	0.0238	0.0235
0.408	0.0277	0.0265

where ϵ_c is the total strain resulting from complete deconvolution. The strain ϵ_c is proportional to the square of the twist and the square of the width of the ribbon. Figure 1 shows how the elongation (due to untwisting) of a thin ribbon increases as the initial twist increases for ribbons of different widths.

For the nylon models which were described in part I, the strain resulting from deconvolution can be calculated from eq. (2) to give the values in Table I. By examining the load-extension curves in Figure 4 of part I, we can get values of ϵ_c similar to those calculated. These values are found by determining the point at which a line tangent to the upper portion of the load-extension curve crosses the elongation axis. All of the curves for the twisted structures are shifted along the elongation axis by an amount equal to ϵ_c . Agreement with calculated values is not expected to be exact, since there are errors of measurement and cutting of the strips.

Cotton Fiber

Ideally we can think of the cotton fiber as a perfect flat ribbon and then use eq. (2) to predict the extensibility due to the deconvolution effect.

Hebert et al.⁵ have shown that the measured x-ray spiral angle Ω is related to the convolution angle ω_0 by the equation

$$\Omega = 0.965\omega_0 + 18.94^\circ \quad (3)$$

If we use this relation and convert the x-ray angles in the data of Orr et al.⁶ to convolution angles and then plot these convolution angles against the observed elongation for the 33 varieties of cotton given, we get the array of points shown in Figure 2. There is no linear relationship between elongation and the convolution angles found by Hebert's equation given above.

As the convolution angle decreases, the points begin to level off at a strain of about 0.065. By examining several sets of data found in the literature in a similar manner, it can be shown that the points are on a curved line, but they can, as a group, be shifted to a different position along the x or y axis. These differences are probably due to the test method used and the method of measuring the x-ray angle.

We know that at the time of fracture, the total fiber strain ϵ would be equal to $\epsilon_s + \epsilon_c$, where ϵ_s is the strain resulting from changes in the fibrillar structure and ϵ_c is the strain from the deconvolution effect. It was shown earlier that if the convolutions are removed by a water treatment, the elongation to break is similar for the four varieties of cotton tested. The leveling of the points in Figure 2 on the fibers with low twist is probably equal to or nearly equal to a value for ϵ_s , although in this case the value of ϵ_s seems too high.

Meredith⁷ has given the following relation for the convolution angle ω_0 :

$$\tan \omega_0 = \pi b/2c \quad (4)$$

where b is the ribbon width and c is the pitch of the convolution (for a rotation of 180°). If ϕ_0 is the twist in radians/unit length, $c = \pi/\phi_0$, then by substituting into eq. (3), it is found that

$$\phi_0 = 2 \tan \omega_0/b \quad (5)$$

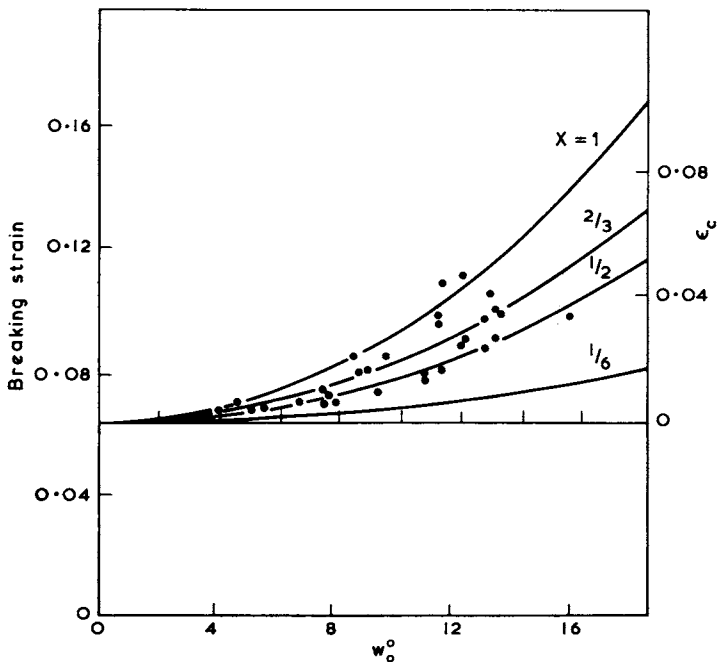


Fig. 2. Experimental results for the relation between breaking strain and convolution angle (points) compared with predicted values of deconvolution strain (lines).

By substituting eq. (5) into (2), we find that

$$\epsilon_c = \frac{1}{6} \tan^2 \omega_0 \quad (6)$$

In practice the cotton fiber will have a variable ω_0 along its length, unequal lengths of S and Z twist, some fibers more circular than ribbon shaped, and some fibers in the wrapped form instead of the twisted form. (Strain resulting from unwrapping would be greater than a simple untwisting.) All of these factors will contribute to a decrease or an increase in the extensibility of the fiber.

If we assume that the form of eq. (6) can be applied to the cotton fiber, but with a different numerical factor, we can write the equation as

$$\epsilon_c = X \tan^2 \omega_0 \quad (7)$$

where X is a factor taking into account the differences mentioned in the last paragraph. Figure 2 shows the relation between ω_0 and ϵ_c with varying values for X , superimposed to fit the experimental results by shifting the zero position of the ϵ_c axis up to a value of $\epsilon = 0.065$. There is reasonable agreement between the two graphs when X is between 0.5 and 1.0.

Mechanics of Deconvolution

The previous sections refer only to the geometrical consequences of complete deconvolution. The extent of deconvolution under a given load remains to be found. An approximate analysis of deconvolution mechanics is given in Appendix I and leads to the result

$$\text{Stress} = f = K \left(\frac{\tan \omega_0}{(\tan^2 \omega_0 - \epsilon_c/X)^{1/2}} - 1 \right) \quad (8)$$

where $K = (gAS_f/\pi b^2X)$ is a factor dependent on the shear modulus of the fiber S_f , the ribbon width b , the area of cross section A , X in eq. (1), and a shape factor g , which approaches 1 from lower values as the fiber becomes more circular.

An estimate of the value of K can be obtained from the data on cross-sectional dimensions obtained by House⁸ and on torsional properties by Meredith⁹ for a number of cottons. Average values of the parameters are

$$g = 0.56$$

$$A/b^2 = 0.27$$

$$S_f = 250 \text{ kg/mm}^2$$

From the results in Figure 2, X appears to be about 0.67, and thus we get $K = 18 \text{ kg/mm}^2$. However, all the parameters will vary with cotton types and conditions, and so a wide range of values of K can be expected.

Figure 3(a) shows that the variation of deconvolution strain with stress for various values of K with a convolution angle of 14° , and Figure 3(b) shows values for various convolution angles with $K = 20$. The important features to note are (1) that for low values of K , most of the deconvolution occurs at low stress and a concave relation is obtained, and (2) that a large increase in the deconvolution strain accompanies the convolution angle.

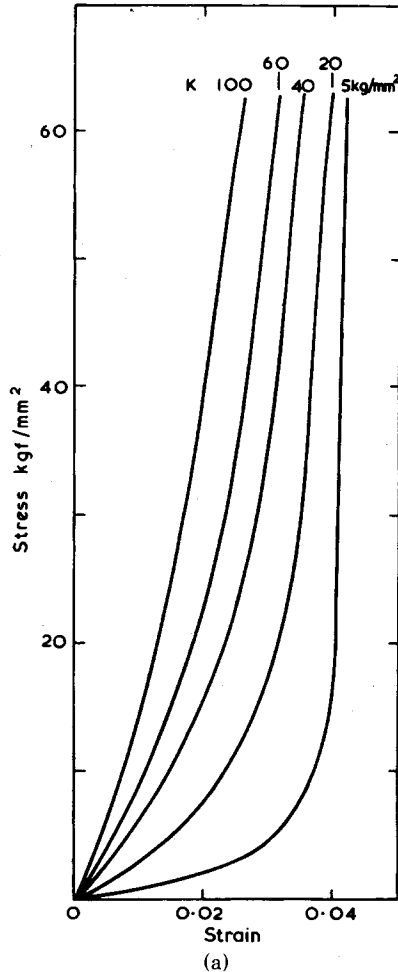


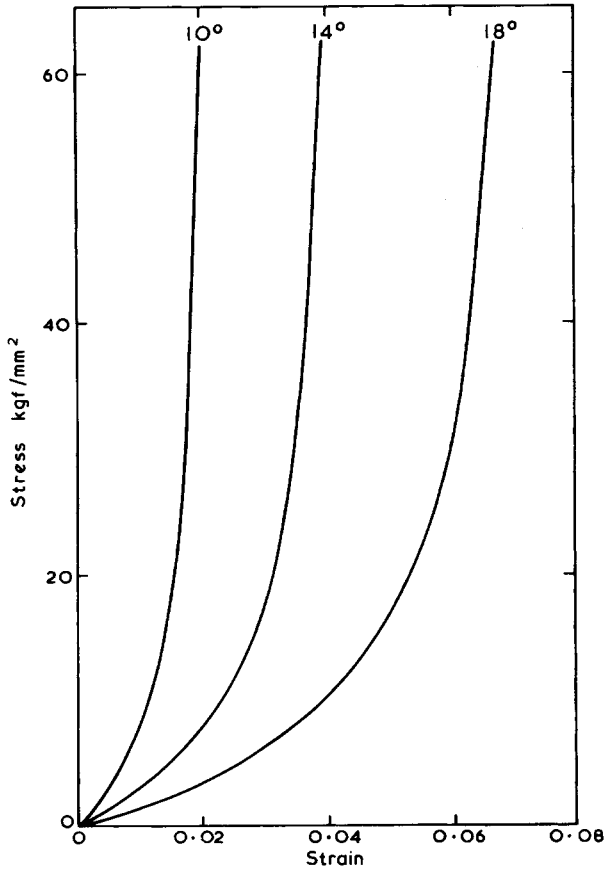
Fig. 3. Variation of deconvolution strain with stress: (a) for $\omega_0 = 14^\circ$ with various values of K ; (b) for $K = 20$ with various values of ω_0 .

THEORETICAL ANALYSIS OF THE HELICAL STRUCTURE

General Method and First Attempts

The model to be analyzed is a circular cylinder in which crystalline material spirals around the axis with a helix angle θ (Fig. 4). The factors which come into the analysis are given in Table II. Since the geometry is similar throughout the cylinder, only a single element at radial distance r , axial length h , and helix length l need be considered. Furthermore, if the situation is limited to small strains and Hookean deformation, all energy terms must be proportional to squares of strains. As stress is increased, all strains must increase proportionately. Whatever analysis is adopted, the final result must follow Hooke's law, and so we are only concerned with calculating values of fiber modulus E .

Not all the factors listed in Table II are brought into every treatment (and a complete analysis would involve still more factors). In any particular case, the method of analysis is to calculate the energies in terms of the geometric variables,



(b)

Fig. 3. (Continued from previous page.)

TABLE II
Factors in Analysis

Independent geometric variable: length h
Dependent geometric variables: radius r and rotation p
Strain energy terms (with related moduli): fibril extensions (Young's modulus E_f), volume change (bulk modulus K_f), and shear (shear modulus S_f)
"Stresses": tensile stress f and torque T

determine the dependent geometric variables by minimizing the total strain energy, and then use the conservation of energy in a virtual change of the independent geometric variable to obtain the associated stress.

By taking into account extension and volume changes but ignoring shear and rotation, Hearle² derived the equation

$$E = E_f(\cos^2 \theta - \sigma \sin^2 \theta)^2 + K_f(1 - 2\sigma)^2 \quad (9)$$

where σ is the fiber Poisson ratio (related to change in radius r). If the bulk modulus K_f is large, there will be no volume change, σ will be 0.5, and eq. (9) becomes

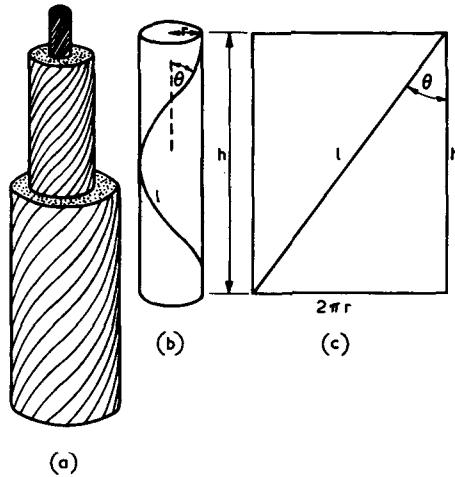


Fig. 4. Helical model: (a) whole system; (b) one turn of a single element; (c) "opened-out" diagram.

$$E = E_f(\cos^2 \theta - \frac{1}{2} \sin^2 \theta)^2 \quad (10)$$

This equation gives a reasonable fit to results for cotton, sisal, and coir,² although the experimental cotton values show a lot of scatter about the theoretical line. Meredith¹⁰ has also shown that it fits results for the dynamic modulus of stretched mercerized cotton fibers.

However, the axial extension and lateral contraction cause a change in helix angle, which implies that the material is sheared, and in a solid material this is not relieved by slippage as it is between the fibers in a yarn. It must therefore contribute an additional energy term. Appendix B modifies the previous analysis given by Hearle² in order to bring in the shear energy (without volume change) and leads to the following equation:

$$E = E_f[(\cos^2 \theta - \sigma \sin^2 \theta)^2 + (S_f/E_f)(1 + \sigma)^2 \sin^2 \theta \cos^2 \theta] \quad (11)$$

Jawson et al.¹¹ have calculated that the shear modulus of crystalline cellulose should be between 36 and 672 kg/mm², and Treloar¹² has calculated Young's modulus along the chain axis to be 5770 kg/mm². Using these values, with σ about 0.5 and θ about 22°, it is found that

$$(S_f/E_f)(1 + \sigma)^2 \sin^2 \theta \cos^2 \theta \ll (\cos^2 \theta - \sigma \sin^2 \theta)^2$$

Consequently the influence of the resistance to shear can be neglected and eq. (10) used. It will apply in circumstances where rotation of the fiber is prevented, as would happen on short test lengths of cotton without a reversal, and in other fibers without reversals or freedom of rotation.

Model with Free Rotation

In cotton fibers, untwisting can occur at reversals during extension. Appendix C gives the analysis which takes this into account and results in the equation

$$E = \frac{E_f S_f \cos^2 \theta}{E_f \sin^2 \theta + S_f \cos^2 \theta} \quad (12)$$

Through a curious trick of the mathematics, it turns out that the minimum of the tensile and torsional energy occurs at constant volume, so that the deformation necessarily occurs with $\sigma = 1/2$, independent of the value of the bulk modulus. We note the dependence on shear modulus, with the modulus dropping to zero as S_f goes to zero. The latter effect must occur, since, with no shear resistance, untwisting can accommodate the length change. In other circumstances there will be a balance between the shear strain energy associated with untwisting and the extension energy change.

Figure 5 shows the variation of fiber modulus with helix angle for various values of shear modulus. The general trend of results is similar to that for Hearle's earlier equation,¹² also shown in Figure 5, though decreasing more rapidly for small spiral angles. In order to make eq. (10) fit, it was necessary to put the fibril Young's modulus equal to 2300 kg/mm² instead of Treloar's theoretical value of 5700 kg/mm². However, if the shear modulus is put within the range of 36–672 kg/mm², then eq. (12) would give a reasonable fit to the experimental results when Young's modulus is 5700 kg/mm²: the most likely value of S_f would be about 200 kg/mm², based on the results for sisal, though the cotton results suggest a higher value.

Figure 6 shows the large variation of fiber modulus with shear modulus for a

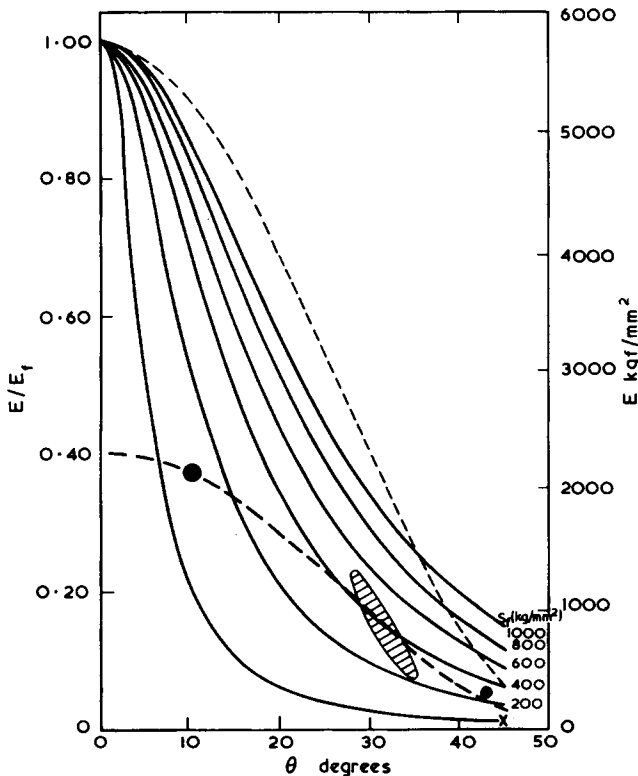


Fig. 5. Variation of modulus E with spiral angle θ . The full lines are for eq. (11) with various values of shear modulus S_f . The dotted lines are for eq. (10). Except for the lower dotted lines, the absolute values are based on $E_f = 5700$ kg/mm² as calculated by Treloar (Ref. 10). The lower dotted line is based on $E_f = 2300$ kg/mm², as used by Hearle (Ref. 2) to fit experimental results for sisal (●), coir (×), and cotton (shaded area).

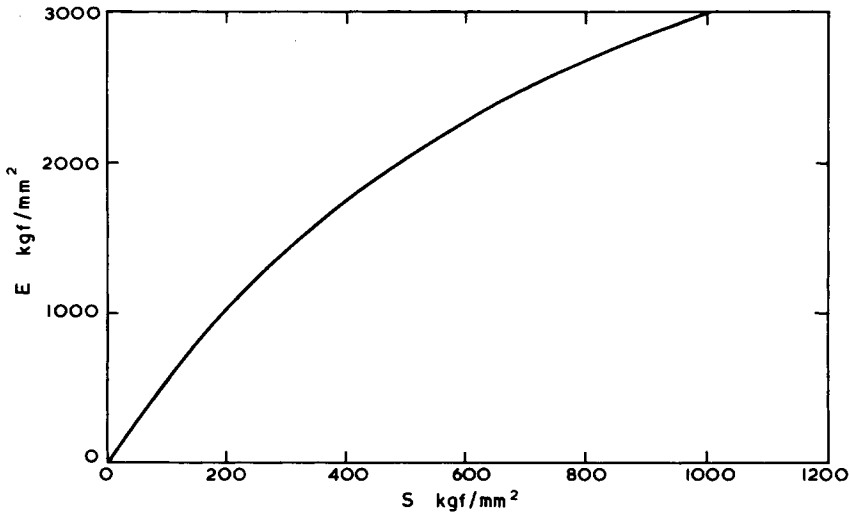


Fig. 6. Variation of fiber modulus with shear modulus for eq. (12) for a spiral angle of 22° with $E_f = 5770 \text{ kg/mm}^2$.

spiral angle of 22° . We can use this to explain the influence of moisture on the tensile stiffness of cotton fibers. Although the tensile modulus of crystalline cellulose would not alter, the shear modulus, which reflects interfibrillar bonding, will be considerably affected. Peirce¹³ has shown that the torsional rigidity of cotton, which depends on shear modulus, does decrease rapidly with moisture regain and can be related simply to the directly absorbed water, which breaks hydrogen bonds between cellulose molecules. Similarly, if the fiber is chemically crosslinked, the shear modulus will be higher and the fiber will be stiffer.

We can also examine the quantitative value of modulus. Taking Jawson's high value of 672 kg/mm^2 for S_f and 5770 kg/mm^2 for E_f , we get a value of 2400 kg/mm^2 for the modulus of an unconvoluted fiber with a spiral angle of 22° . In order to compare this with experiments, we can use Hebert's equation (3) as before to convert the spiral angle to the convolution angle in Meredith's data¹⁴ and so plot initial modulus against convolution angle (Fig. 7). Extrapolation to zero convolution angle gives a modulus of 2300 kg/mm^2 , which agrees well with the predicted value.

Combined Effect of Deconvolution and Deformation of the Helical Assembly

We have now considered separately the two effects of (1) a convoluted ribbon-shaped fiber with convolution reversals and (2) a cylindrical fiber with a reversing helical assembly of fibrils. A full treatment, which would require an analysis of the combined situations, would be very difficult. We therefore need to look for an approximate means of combining them. Under stress, both effects, deconvolution and deformation of the assembly, will occur, and we therefore add together the strains due to each mechanism.

Taking 2400 kg/mm^2 as the modulus of the unconvoluted fiber and combining the strains ϵ_s from this line with that of the deconvolution effect ϵ_c , we can begin to get a reasonable approximation, $\epsilon_s + \epsilon_c$, for the stress-strain behavior of the

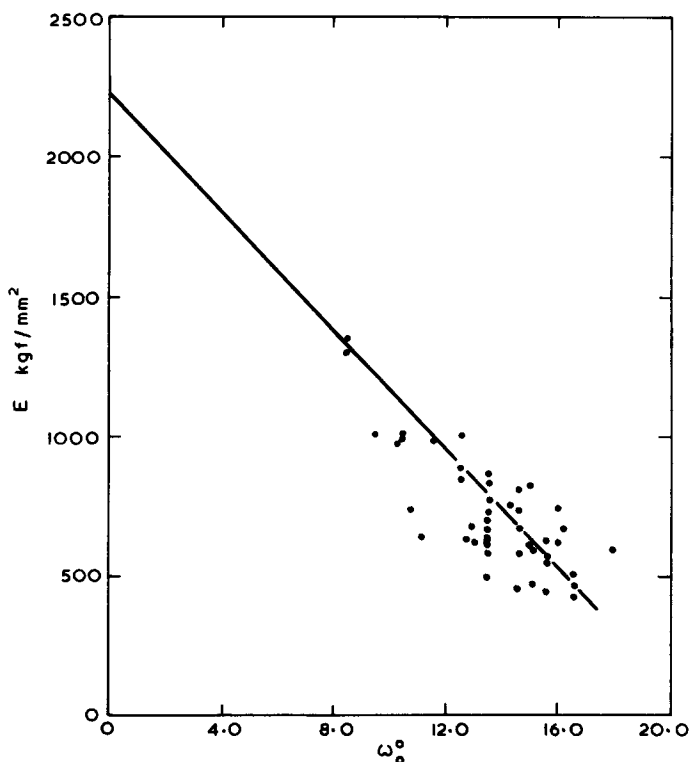


Fig. 7. Variation of cotton fiber modulus with convolution angle, for Meredith's data (Ref. 12) on modulus and x-ray angle, transformed by Hebert's eq. (3).

cotton fiber (Fig. 8). In this case we have given the fiber a convolution angle of 14° and K , from eq. (8), a value of 2.0, which is not unreasonable for a fiber at 65% R.H.

As a comparison with experimental results, Figure 9 shows stress-strain curves found by Meredith¹⁵ for a high-modulus St. Vincent cotton and a low-modulus Ishan cotton. The theoretical line for $\epsilon_s + \epsilon_c$ initially falls below both curves, indicating a rather stronger resistance to deconvolution in the actual fibers and then lies between them. A fairly modest change of what are rather roughly estimated parameters would bring good agreement. Also shown in Figure 9 is the close agreement between ϵ_s , which is the effect of the helical assembly without convolutions, and the stress-strain curve of one of the cotton fibers which has been stretched and set in water, as described in part I, in order to remove convolutions.

Figure 10 shows how moisture might affect the stress-strain curve, although the numerical values selected are purely illustrative and do not have any real justification. Curves b, e, and h are the curves in Figure 8 which are assumed to be correct values of ϵ_s , ϵ_c , and $\epsilon_s + \epsilon_c$, respectively, for a cotton fiber at 65% R.H. For ϵ_s at low and high humidities, we now take lines a and c with higher and lower moduli as given in Table III. The effect of moisture in lowering the shear modulus of the fiber will also make deconvolution easier and reduce the value of K . However, it will also decrease the convolution angle. Possible combinations are shown in Table III and these give the curves d and f in Figure

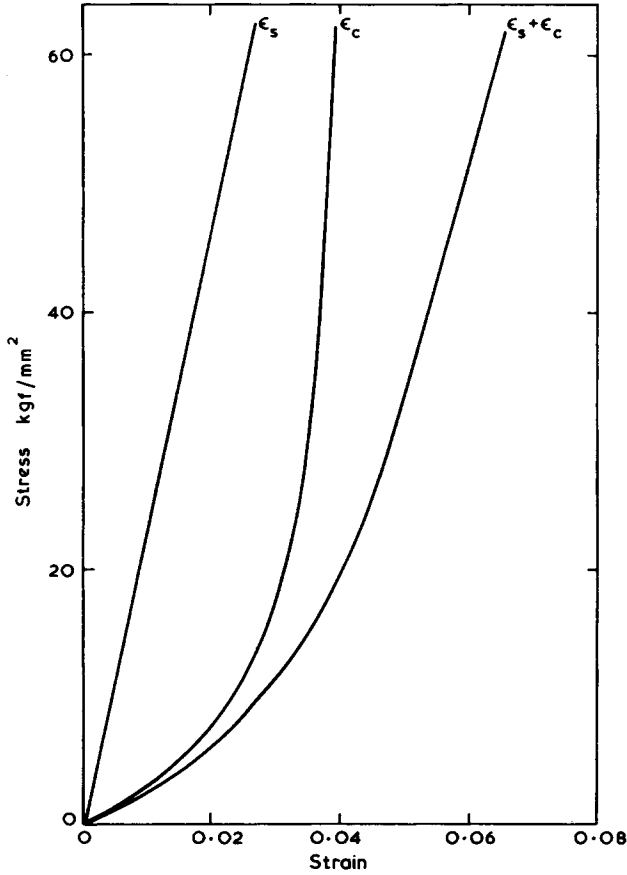


Fig. 8. Combination of deconvolution strain ϵ_c with helical deformation strain ϵ_s to give total strain ($\epsilon_s + \epsilon_c$).

TABLE III
Illustrative Values for Different Humidities Taken from Fig. 10

Curve	Low R.H.			Medium R.H.			High R.H.		
	$E, \text{kg/mm}^2$	K	ω_0, deg	$E, \text{kg/mm}^2$	K	ω_0, deg	$E, \text{kg/mm}^2$	K	ω_0, deg
a	4400								
b				2400					
c							1200		
d		60	16°						
e					20	14°			
f								5	12°

10. Addition gives the lines g and i for the total strain. Furthermore, if it is assumed that the higher shear stress leads to earlier fracture, then the strength would change as indicated. The curves g, h, and i are in general agreement with those found experimentally for cotton at 0, 65, and 100% R.H. by Meredith.¹⁶ No doubt a very close fit could be obtained by a suitable choice of parameters, but it is not worth trying this without independent evidence of the value of parameters.

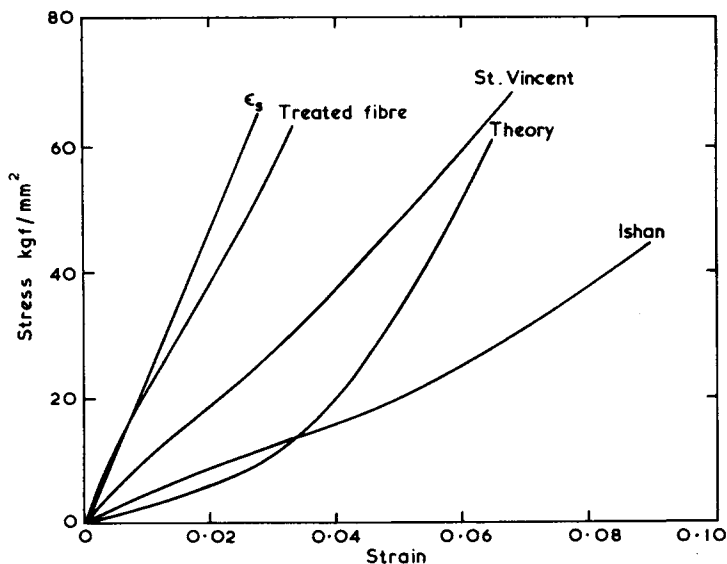


Fig. 9. Theoretical stress-strain curves for $\epsilon_s + \epsilon_c$ compared with experimental results for St. Vincent and Ishan cottons and ϵ_s compared with results for set stretched cotton fiber.

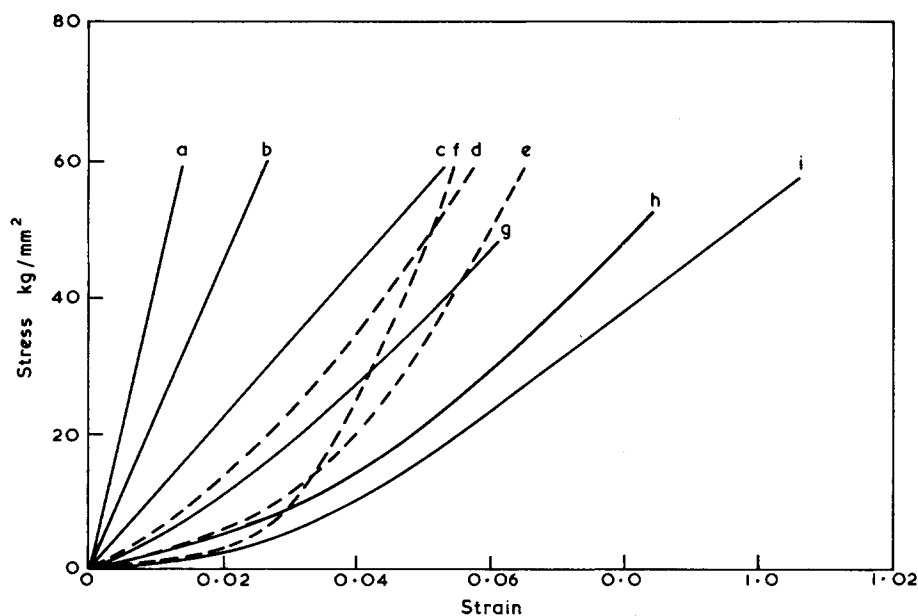


Fig. 10. Stress-strain curves at low humidity: a, ϵ_s ; d, ϵ_c ; g, ($\epsilon_s + \epsilon_c$); medium humidity: b, ϵ_s ; e, ϵ_c ; h, $\epsilon_s + \epsilon_c$; and high humidity: c, ϵ_s ; f, ϵ_c ; i, $\epsilon_s + \epsilon_c$. (Values of parameters in Table III.)

CONCLUSION

In part I we showed experimentally the importance of deconvolution in contributing to cotton fiber extension, and in this paper we have quantified the effect. In addition, a new analysis of the extension of the helical assembly has been carried out in order to allow for the false untwisting which can occur at reversal points. An important consequence of the latter effect is that the associated fiber

modulus is strongly dependent on the fiber shear modulus. Since Clayton and Peirce¹⁷ have shown that the shear modulus of cotton can fall by 10 times between 0 and 100% R.H., the large effect of moisture on tensile properties is explained. The resistance to deconvolution will also be affected by the change in stiffness. Any feature such as resin crosslinking which increases the shear modulus (or rather prevents its decrease with relative humidity) will also have the effect of stiffening the fiber.

The combination of the deconvolution with deformation of the helical assembly yields stress-strain curves of the same shape as those of cotton fibers and, when plausible values of parameters are inserted, of the right order of magnitude.

It seems certain that the mechanisms described in this paper, namely, deconvolution due to untwisting or unbending of the convolutions plus an extension of the helical assembly with free untwisting at reversals, are the dominant factors in cotton fiber extension. It is possible that a fresh study of different cotton fibers under various moisture conditions and chemical treatments that measured both the stress-strain curves and dynamic moduli at various strains—along with a careful attempt to measure the relevant parameters with, perhaps a further refinement of the theory—might serve to show even closer agreement. However, this would seem to be an academic exercise which would be unlikely to yield greater understanding.

From a practical point of view, the importance of the work is in showing the nature of the influence of tensile modulus, shear modulus, spiral angle, and convolution geometry on cotton fiber mechanical properties. The tensile modulus is not likely to be amenable to change, but the shear modulus, spiral angle, and convolution geometry can be changed by previous chemical treatments and by the environment of the fibers. A closer look at these effects in the light of the knowledge of the mechanics and the practical needs might be of value. It seems unlikely that the moduli can be changed by plant breeding, and the spiral angle also seems remarkably constant, though there has probably not been any attempt to breed selectively for true spiral angle. The convolution geometry certainly varies between cotton varieties and could be examined in relation to selection.

We acknowledge the financial assistance and the advice of the International Institute for Cotton.

APPENDIX A: MECHANICS OF THE DECONVOLUTION

A rough analysis of the stress-strain behavior in deconvolution can be made by assuming that the energy involved is the energy of untwisting and that the axial strain is given by eq. (7) derived from Timoshenko's relation (1).

If a fiber with an initial twist ϕ_0 radians/unit length is untwisted to ϕ , then the standard treatment, given for example by Morton and Hearle,¹⁸ shows that

$$\text{torque} = T = gA^2S_f(\phi_0 - \phi)/2\pi$$

where g is a shape factor equal to 1 for a circle, A is the fiber area, and S_f is fiber shear modulus, and

$$\begin{aligned} \text{energy/unit volume} &= U = \frac{1}{2} \text{torque} \times \text{twist/volume} \\ &= gAS_f(\phi_0 - \phi)^2/4\pi \\ &= gAS_f(\phi_0^2 - 2\phi_0\phi + \phi^2)/4\pi \end{aligned}$$

From eq. (5) we have

$$\phi_0 = 2 \tan(\omega_0/b), \quad \phi = 2 \tan(\omega/b)$$

and from eq. (7) the deconvolution strain ϵ_c is given by

$$\epsilon_c = X(\tan^2 \omega_0 - \tan^2 \omega)$$

Thus

$$\tan \omega = (\tan^2 \omega_0 - \epsilon_c/X)^{1/2}$$

Hence

$$U = \frac{gAS_f}{\pi b^2} [\tan^2 \omega_0 - 2 \tan \omega_0(\tan^2 \omega_0 - \epsilon_c/X)^{1/2} + \tan^2 \omega_0 - \epsilon_c/X]$$

$$\text{Stress} = f = \frac{dU}{d\epsilon_c} = \frac{gAS_f}{\pi b^2 X} \left(\frac{\tan \omega_0}{(\tan^2 \omega_0 - \epsilon_c/X)^{1/2}} \right)$$

APPENDIX B: MODIFICATION OF PREVIOUS ANALYSIS (2) TO ALLOW FOR SHEAR ENERGY

Figure 11 shows the “opened-out” diagram of Figure 4 with a tensile strain ϵ and a transverse strain ($-\sigma\epsilon$). It is clear from the diagram that there is shear associated with the angular change. We see that

$$\text{shear strain} = \beta = d\theta$$

From the geometry, we have

$$\begin{aligned} \tan \theta &= 2\pi r/h \\ \sec^2 \theta d\theta &= 2\pi \frac{dr}{h} - 2\pi r \frac{dh}{h^2} \\ \beta = d\theta &= \frac{\tan \theta}{\sec^2 \theta} \frac{dr}{r} - \frac{dh}{h} = (\sin \theta \cos \theta)(-\sigma\epsilon - \epsilon) \\ \text{shear energy} = U_1 &= \frac{1}{2} S_f \beta^2 \\ &= \frac{1}{2} S_f (1 + \sigma)^2 \sin^2 \theta \cos^2 \theta \epsilon^2 \end{aligned}$$

From the earlier analysis (2), we have

$$\text{energy of fibril extension} = \frac{1}{2} E_f \epsilon_f^2$$

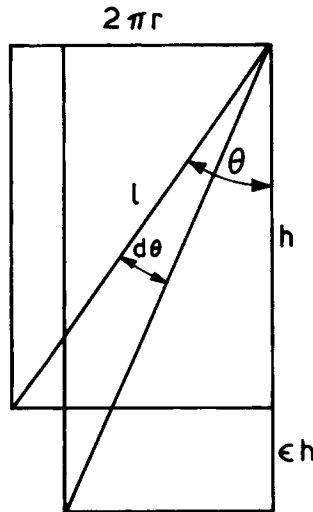


Fig. 11. Cylindrical helical geometry opened out flat.

$$= \frac{1}{2} E_f \epsilon^2 (\cos^2 \theta - \sigma \sin^2 \theta)^2$$

If it is assumed that there is no appreciable volume change, we have

$$\begin{aligned} \text{total energy} = U &= U_1 + U_2 \\ &= \frac{1}{2} \epsilon^2 [E_f (\cos^2 \theta - \sigma \sin^2 \theta)^2 + S_f (1 + \sigma)^2 \sin^2 \theta \cos^2 \theta] \end{aligned}$$

Consequently

$$\text{Modulus} = E = E_f (\cos^2 \theta - \sigma \sin^2 \theta)^2 + S_f (1 + \sigma)^2 \sin^2 \theta \cos^2 \theta$$

APPENDIX C: EXTENSION OF HELICAL ASSEMBLY WITH FREE UNTWISTING

If there is no resistance to untwisting (either through free ends or at reversal points in alternating twist), the number of turns in a given piece changes and so h cannot be taken as the length corresponding to one turn as is usual in yarn mechanics. Instead we consider an element, as in Figure 12, in which there are p turns in the unstrained state. The arc length is then $p(2\pi r)$. For the overall fiber deformation, we put

$$\begin{aligned} \text{fiber strain} &= \frac{dh}{h} = \epsilon \\ \text{transverse strain} &= \frac{dr}{r} = -\sigma \epsilon \\ \text{rotational change} &= \frac{dp}{p} = -\gamma \epsilon \end{aligned}$$

where γ is a parameter relating untwisting to extension, analogous to a Poisson ratio.

From the Pythagorean theorem we have

$$\begin{aligned} l^2 &= h^2 + p^2(4\pi^2 r^2) \\ 2l \, dl &= 2h \, dh + 2p \, dp(4\pi^2 r^2) + p^2(4\pi^2 r \, dr) \end{aligned}$$

Therefore,

$$\begin{aligned} \text{fibril extension} = \epsilon_f &= \frac{dl}{l} \\ &= \frac{h^2 dh}{l^2 h} + \frac{p^2(4\pi^2 r^2) dp}{l^2 p} + \frac{p^2(2\pi^2 r^2) dr}{l^2 r} \\ \epsilon_f &= \epsilon [\cos^2 \theta - (\gamma + \sigma) \sin^2 \theta] \end{aligned}$$

There will be an energy term U_1 (per unit volume) associated with fibril extension and the fiber modulus E_f :

$$U_1 = \frac{1}{2} E_f \epsilon_f^2 = \frac{1}{2} E_f \epsilon^2 [\cos^2 \theta - (\gamma + \sigma) \sin^2 \theta]^2$$

Next we have

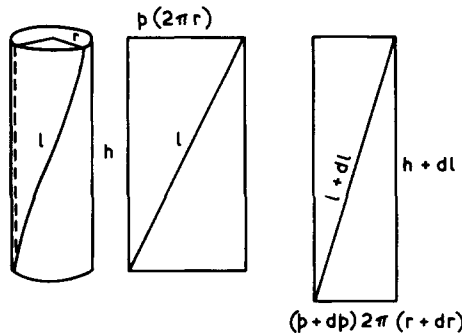


Fig. 12. Element with a fraction p of one turn.

$$\begin{aligned}\text{volume of element} &= V = \pi r^2 h \\ dV &= \pi r^2 dh + 2\pi r h dr \\ \text{volume strain} &= \frac{dV}{V} \\ &= \frac{dh}{h} + \frac{2 dr}{r} = \epsilon - 2\sigma\epsilon\end{aligned}$$

This gives a volume energy term U_2 , dependent on the bulk modulus K .

$$U_2 = \frac{1}{2} K_f \left(\frac{dV}{V} \right)^2 = \frac{1}{2} K_f \epsilon^2 (1 - 2\sigma)^2$$

The change in fibril angle gives a shear strain $d\theta$. From the triangle we have

$$\begin{aligned}h \tan \theta &= p(2\pi r) \\ \tan \theta dh + h \sec^2 \theta d\theta &= 2\pi r dp + 2\pi p dr\end{aligned}$$

Dividing the second equation by the first, we find

$$\frac{dh}{h} + \frac{\sec^2 \theta d\theta}{\tan \theta} = \frac{dp}{p} + \frac{dr}{r}$$

Hence

$$d\theta = \epsilon \sin \theta \cos \theta (-\gamma - \sigma - 1)$$

The shear energy terms U_3 , associated with the shear modulus S_f , is given by

$$\begin{aligned}U_3 &= \frac{1}{2} S_f (d\theta)^2 \\ &= \frac{1}{2} S_f \epsilon^2 \sin^2 \theta \cos^2 \theta (\gamma + \sigma + 1)^2\end{aligned}$$

(The sign change is convenient and possible in a squared term.)

The total elastic energy U is given by

$$\begin{aligned}U &= U_1 + U_2 + U_3 \\ &= \frac{1}{2} \epsilon^2 \{ E_f [\cos^2 \theta - (\gamma + \sigma) \sin^2 \theta]^2 + K_f (1 - 2\sigma)^2 + S_f \sin^2 \theta \cos^2 \theta (\gamma + \sigma + 1)^2 \}\end{aligned}$$

Hence the term in the brackets $\{ \}$ is the fiber modulus.

The transverse contraction and the rotation will adjust freely to give a minimum of energy. Therefore, we have

$$\begin{aligned}\left(\frac{\partial U}{\partial \sigma} \right)_{\epsilon, \gamma} &= \epsilon^2 \{ E_f [\cos^2 \theta - (\gamma + \sigma) \sin^2 \theta] (-\sin^2 \theta) + K_f (1 - 2\sigma) (-2) + S_f \sin^2 \theta \cos^2 \theta (\gamma + \sigma + 1) \} \\ &= 0\end{aligned}$$

$$\sigma = - \frac{(E_f - S_f - \gamma S_f) \sin^2 \theta \cos^2 \theta - \gamma E_f \sin^4 \theta + 2K_f}{E_f \sin^4 \theta + S_f \sin^2 \theta \cos^2 \theta + 4K_f}$$

$$\begin{aligned}\left(\frac{\partial U}{\partial \gamma} \right)_{\epsilon, \sigma} &= \epsilon^2 \{ E_f [\cos^2 \theta - (\gamma + \sigma) \sin^2 \theta] (-\sin^2 \theta) + S_f \sin^2 \theta \cos^2 \theta (\gamma + \sigma + 1) \} \\ &= 0\end{aligned}$$

$$\sigma = \frac{(E_f - S_f) \cos^2 \theta - \gamma (E_f \sin^2 \theta + S_f \cos^2 \theta)}{E_f \sin^2 \theta + S_f \cos^2 \theta}$$

If we solve these two expressions for σ simultaneously, we get

$$\begin{aligned}\sigma &= 1/2 \\ \gamma &= \frac{(E_f - S_f) \cos^2 \theta}{E_f \sin^2 \theta + S_f \cos^2 \theta} - \frac{1}{2}\end{aligned}$$

Remarkably, when free untwisting is allowed, the deformation occurs at constant volume, whatever

the value of the bulk modulus, which does not occur in the final equations. Substitution in the expression in brackets {} for the modulus gives

$$E = \frac{E_f S_f \cos^2 \theta}{E_f \sin^2 \theta + S_f \cos^2 \theta}$$

References

1. J. W. S. Hearle, *J. Appl. Polym. Sci.*, **7**, 1207 (1963).
2. J. W. S. Hearle, *J. Polym. Sci. Part C*, **20**, 615 (1967).
3. J. W. S. Hearle and M. Konopasek, *J. Appl. Polym. Sci. Polym. Symp.* **27**, 253 (1975).
4. S. Timoshenko, *Strength of Materials*, Part II, Van Nostrand, New York, 1957, p. 259.
5. J. J. Hebert, R. Giardina, D. Mitcham, and M. L. Rollins, *Text. Res. J.*, **40**, 126 (1970).
6. R. S. Orr, A. W. Burgis, L. B. Deluca, and J. N. Grant, *Text. Res. J.*, **31**, 302 (1961).
7. R. Meredith, *J. Text. Inst.*, **42**, T291 (1951).
8. D. L. House, M.Sc. thesis, Georgia Institute of Technology, 1966.
9. R. Meredith, *J. Text. Inst.*, **45**, T489 (1954).
10. R. Meredith, *Proceedings of the Fifth International Congress of Rheology, Vol. 1*, University of Tokyo Press, 1969, p. 43.
11. M. A. Jawson, P. P. Giles, and R. E. Mark, *Proc. R. Soc. London, Ser. A*, **306**, 389 (1968).
12. L. R. G. Treloar, *Polymer*, **1**, 290 (1960).
13. F. T. Peirce, *J. Text. Inst.*, **20**, T133 (1929).
14. R. Meredith, *J. Text. Inst.*, **37**, T209 (1946).
15. R. Meredith, *J. Text. Inst.*, **36**, T107 (1945).
16. R. Meredith, in *Fibre Science, 2nd ed.*, J. M. Preston, Ed., Textile Institute, London, 1953, p. 252.
17. F. H. Clayton and F. T. Peirce, *J. Text. Inst.*, **20**, T315 (1929).
18. W. E. Morton and J. W. S. Hearle, *Physical Properties of Textile Fibres*, Heinemann and Textile Institute, London, 1975, p. 410.

Received November 14, 1978